Journal of Alloys and Compounds 509 (2011) 8794–8797

Contents lists available at ScienceDirect

Journal of Alloys and Compounds

journal homepage: www.elsevier.com/locate/jallcom

Enhanced sintering, microstructure evolution and mechanical properties of 316L stainless steel with $MoSi_2$ addition

Farid Akhtar[a,b,*], Liaqat Ali[b], Feng Peizhong[c], Jawad Ali Shah[b]

[a] Department of Materials and Environmental Chemistry, Stockholm University, Stockholm 10691, Sweden
[b] Department of Metallurgical and Materials Engineering, University of Engineering and Technology, Lahore 54890, Pakistan
[c] School of Materials Science and Engineering, China University of Mining and Technology, Xuzhou 221116, PR China

ARTICLE INFO

Article history:
Received 25 May 2011
Received in revised form 13 June 2011
Accepted 16 June 2011
Available online 23 June 2011

Keywords:
316L stainless steel
Sintering
$MoSi_2$
Microstructure
XMAP
Mechanical properties

ABSTRACT

Sintering 316L stainless steel to near full density with an appropriate sintering additive can ensure high mechanical properties and corrosion resistance. We present here a sintering approach which exploits the dissociation of ceramics in steels at high temperatures to activate sintering densification to achieve near full dense 316L stainless steel materials. $MoSi_2$ ceramic powder was used as a sintering additive for pre-alloyed 316L stainless steel powder. Sintering behavior and microstructure evolution were investigated at various sintering temperatures and content of $MoSi_2$ as sintering additive. The results showed that the sintering densification was enhanced with temperature and $MoSi_2$ content. The distribution of $MoSi_2$ was characterized by XMAPs. It was found that $MoSi_2$ dissociated during sintering and Mo and Si segregated at the grain boundaries. Excess Mo and Si were appeared as separate phases in the microstructure. Above 98% of theoretical density was achieved when the specimens were sintered at 1300 °C for 60 min with 5 wt.% $MoSi_2$ content. The stainless steel sintered with 5 wt.% $MoSi_2$ exhibited very attractive mechanical properties.

1. Introduction

Dense 316L stainless steel is widely used in automotive, medical and structural applications. Powder metallurgy (P/M) being a near net shaping process reduces processing cost and is attractive for production of 316L parts [1]. In order to compete with dense 316L parts, high density P/M 316L parts with high mechanical and corrosion properties are required. One of the investigated ways to fabricate high density P/M stainless steel parts is the addition of sintering additives to stainless steel powder [2]. The sintering additives lower the sintering temperature and activate densification mechanisms to eliminate pores. Sintering additives such as FeB, NiB, FeMoB, Si and Cu_3P have been reported for the enhanced sintering of stainless steels [2–8]. These sintering additives activate the sintering process of stainless steel powders by the formation of a liquid phase. The liquid phase forms a network between solid grains and favors the classical phenomenon of liquid phase sintering [3,7].

Choice of a sintering additive is complex and involves the understanding of the complex chemical reactions. Adverse effects like swelling, porosity and dramatic decrease in mechanical and corrosion properties could be observed [9]. So far, few studies have reported the successful incorporation of high volume fraction of ceramic reinforcements to fabricate stainless steel reinforced composites with high density to improve wear resistance [10–12]. On the other hand, low volume fraction of ceramics has been used to enhance sintering densification and to prepare low volume fraction P/M stainless steels particulate composites [13–16]. Sintering of 316L stainless steel powders with up to 10 vol.% YAG addition showed that the sintering porosity was more homogeneous for 5 vol.% YAG containing composite compared to 316L stainless steel under identical sintering conditions [14]. Addition of SiC and Si_3N_4 to stainless steel resulted in higher sintered density. Enhanced sintering with the addition of SiC to 316L was attributed to the interaction of SiC with 316L stainless steel matrix, resulting in formation of a low melting Fe–SiC phase [15]. Si_3N_4 dissociated in the 465 stainless steel in Si and N and resulted in enhanced densification and high mechanical properties [16]. Due to chemical instability of various ceramics and strong bonding while interacting with steels, the addition of ceramics can be exploited as sintering additive and their components could enhance mechanical and corrosion properties. $MoSi_2$ is a ceramic material with high melting point and excellent high temperature oxidation resistance [17,18]. It has been reported theoretically that $MoSi_2$ develops strong bonds with Fe by making Fe–Mo and Fe–Si bonds at the interface [19]. Successful preparation of $MoSi_2$ and 316L joints has been recently reported by so called spark plasma technique. Dissolution of $MoSi_2$ was evidenced during the processing [20]. Hence, it is hypothe-

* Corresponding author at: Department of Materials and Environmental Chemistry, Stockholm University, Stockholm 10691, Sweden.
E-mail address: farid.akhtar@mmk.su.se (F. Akhtar).

0925-8388/$ – see front matter © 2011 Elsevier B.V. All rights reserved.
doi:10.1016/j.jallcom.2011.06.077

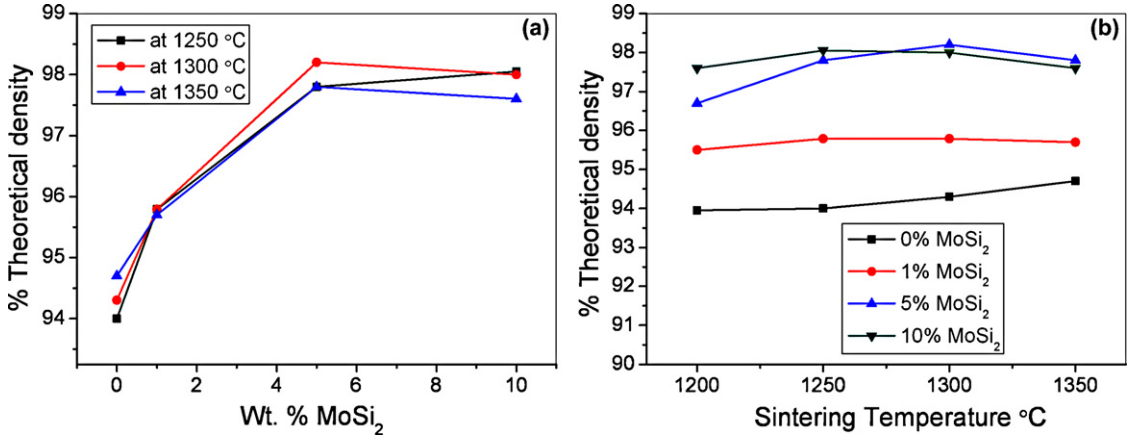

Fig. 1. (a) Effect of $MoSi_2$ addition on the sintered density at 1250, 1300 and 1350 °C for 60 min. (b) Effect of sintering temperature on the sintered density (sintering time 60 min) with 0–10 wt.% $MoSi_2$ addition.

sized that $MoSi_2$ can possibly be used as sintering additive due to its strong interaction and bonding with 316L stainless steel. Mo addition to austenitic steels could enhance the pitting and crevice corrosion especially for the steel containing Cr [21–24] and Si can act as sintering additive to form liquid phase at the sintering temperature to facilitate the densification process [8,25].

The present work investigates the effect of $MoSi_2$ addition on the sintering behavior, microstructure evolution and mechanical properties of P/M 316L stainless steel. The sintering behavior of 316L stainless steel was studied with varying $MoSi_2$ content and at various sintering temperatures. Metallographic techniques were employed to investigate the effect of sintering temperature and $MoSi_2$ addition on the microstructure evolution of P/M 316L stainless steel. The sintering mechanisms will be discussed using electron microscopy and elemental mapping.

2. Experimental

Pre-alloyed 316L powder (37 μm) was dry milled with $MoSi_2$ powder (2 μm) for 6 h. 0, 2, 5 and 10 wt.% $MoSi_2$ was added as sintering additive. EBS wax was added as an inner lubricant. The milled powder was poured into cylindrical die of 10 mm diameter and a tensile specimen die to prepare tensile specimens with 25 mm gauge length and uniaxially pressed at a pressure of 600 MPa.

Sintering of pressed green compacts was performed in a high temperature vacuum furnace with nitrogen back-filling to avoid the evaporation of chromium. The sintering cycle applied to the specimens was as follows: the specimens were heated to 1000 °C at a rate of 10 °C/min and held at 1000 °C for 15 min, then the specimens were heated to various sintering temperatures of 1250 °C, 1300 °C, 1350 °C and 1400 °C at a rate of 5 °C/min and held at each temperature for 60 min in vacuum with nitrogen back-filling. Archimedes water immersion method was employed for the measurement of density of green and sintered specimens. For metallographic examination, the specimens were cut and metallographically polished successively on SiC papers and then fine polished to 0.5 μm diamond finish. The microstructure of sintered specimens and elemental maps was observed on Kevex LEO-1450 SEM operating at 15 kV.

Tensile tests were performed on an Instron mechanical tester at constant crosshead speed of 0.5 mm/min (25 mm gauge length). Tensile specimens were polished successively on SiC papers up to 1000 grit. The hardness test was performed at HRB scale. At least three tests were conducted under the same conditions for reliability of results.

3. Results and discussions

Liquid phase sintering occurs in the presence of liquid phase and powder compacts undergo densification due to rapid material's transport through the liquid phase. Densification rate can increase further with the increase in the liquid volume fraction and decrease in the liquid viscosity, when sintering temperature is increased [26]. The influence of $MoSi_2$ content and sintering temperature on the densification behavior during sintering of 316L stainless steel is summarized in Fig. 1. It can be seen that % theoretical density of 316L stainless steel compacts increases with the addition of $MoSi_2$. With out $MoSi_2$ addition 316L shows high sintered density, 94% of the theoretical, when sintered at 1250 °C. A slight increase in density is observed with increase in sintering temperature to 1350 °C. The effect of $MoSi_2$ addition to 316L stainless steel at various sintering temperatures (Fig. 1) shows that the sintered density increases to 95.6% when 1 wt.% of $MoSi_2$ is added. Highest density, 98.2% of theoretical, is obtained for the specimens sintered at 1300 °C with 5 wt.% $MoSi_2$ addition. Further increase in the density is not observed with increase in temperature and $MoSi_2$ content. Increase in sintered density from 94% to 98.2% of the theoretical is due to the enhanced sintering of specimens with the addition of $MoSi_2$. Hence, it is possible to sinter 316L stainless steel to a high density above 98% of the theoretical with the addition of $MoSi_2$ as high as 5 wt.% at 1300 °C. The effect of $MoSi_2$ addition to 316L stainless steel on the green, ideal and sintered density is summarized in Table 1.

The microstructure of $MoSi_2$ free sintered 316L stainless steel alloy in Fig. 2(a) shows sintered grains and pores inside, similar findings are reported in literature [8,25]. The microstructure of 316L stainless steel with 1 wt.% addition of $MoSi_2$ in Fig. 2(b) shows sintered grains with comparatively (Fig. 2(a)) lower porosity. Considerable reduction in the porosity is visible with the addition of 1 wt.% $MoSi_2$. Further increase in $MoSi_2$ content to 5 wt.% dramatically reduces the porosity and favors grain growth (Fig. 2(c)). The dramatic decrease in the porosity and considerable grain growth clearly evidence the presence of liquid phase during the sintering cycle which facilitates the annihilation of porosity and grain growth by fast mass transport [2,8,25,26]. $MoSi_2$ addition to 316L stainless

Table 1
Effect of $MoSi_2$ addition to 316L stainless steel on the green, theoretical and sintered density (1300 °C).

No.	316L steel (wt.%)	$MoSi_2$ (wt.%)	Green density (g/cm^3)	Theoretical density (g/cm^3)	Sintered density (g/cm^3)	% relative density
1	100.0	0.0	6.41 ± 0.03	7.98	7.52 ± 0.02	94.3
2	99.0	1.0	6.42 ± 0.03	7.97	7.62 ± 0.03	95.6
3	95.0	5.0	6.32 ± 0.02	7.89	7.75 ± 0.02	98.2
4	90.0	10.0	6.27 ± 0.04	7.81	7.64 ± 0.05	98.0

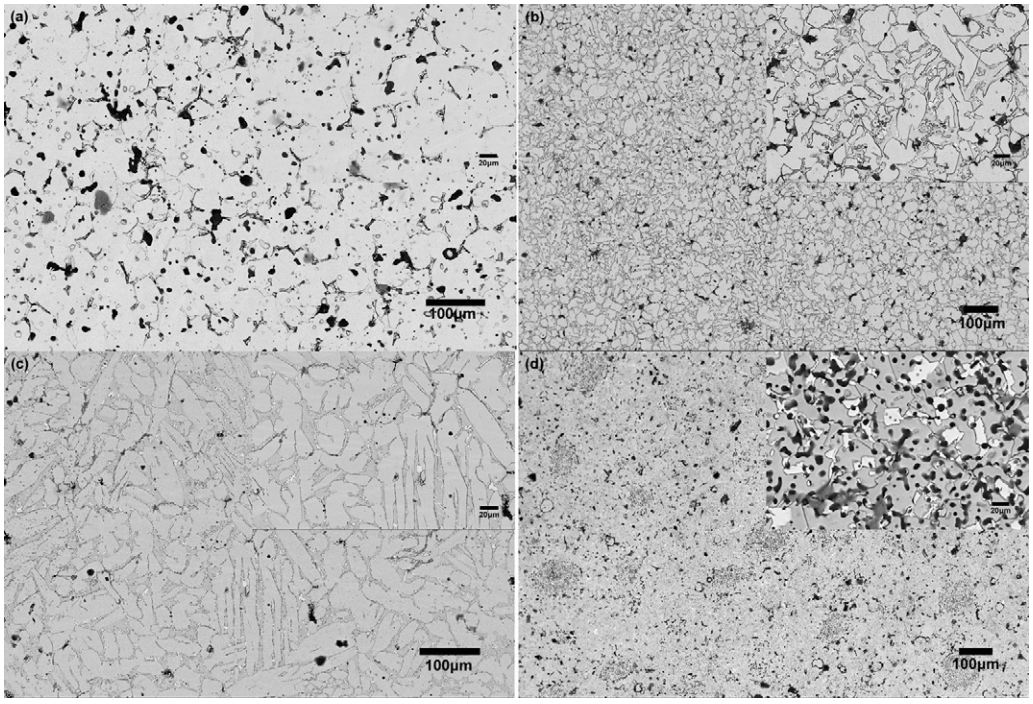

Fig. 2. Microstructures of sintered 316 stainless steel (a) with 0 wt.% $MoSi_2$ addition sintered at 1300 °C for 60 min; (b) with 1 wt.% $MoSi_2$ addition sintered at 1300 °C for 60 min; (c) with 5 wt.% $MoSi_2$ addition sintered at 1300 °C for 60 min; (d) with 10 wt.% $MoSi_2$ sintered at 1300 °C for 60 min.

steel activates the sintering process of steel powders by formation of liquid phase. The liquid phase has low solubility in the stainless steel powder and hence favors the classical phenomenon of liquid phase sintering.

The microstructure of the 316L stainless steel with 10 wt.% $MoSi_2$ addition sintered at 1300 °C in Fig. 2(d) shows the dense sintered structure with the presence of round particles (inset in Fig. 2(d)). The microstructure could be evolved by the dissociation of $MoSi_2$ in to its constituents, Mo and Si. Excessive insoluble molybdenum and silicon can precipitate out from the matrix as a separate phase (inset in Fig. 2(d)). To understand further the sintering mechanisms and evolution of microstructure XMAPs of Mo and Si were obtained from the specimens containing 5 wt.% and 10 wt.% $MoSi_2$. XMAPs of Mo and Si from 316L sintered specimens with 5 wt.% $MoSi_2$ in Fig. 3(a)–(c) shows that $MoSi_2$ has been dissociated in to its constituents Mo and Si during sintering at 1300 °C. Mo segregates along the grain boundaries and Si goes to grain boundaries and matrix. Additions of Si to austenitic stainless steels have been reported to enhance densification during sintering cycle [8,25]. On the other hand, Mo reduces the solubility of C in steels, forms carbides and can effect the corrosion properties at high temperatures [27]. In our case the carbon content is very low in 316L stainless steel (<0.03%), hence we can assume the presence of nearly pure Mo phase in the microstructure. The presence of dispersed Mo phase is beneficial for the mechanical (Table 2) and corrosion properties of sintered stainless steel [23,24,28].

$MoSi_2$ dissociates in 316 stainless steel alloys and Mo appears as a separate phase shows the low solubility of Mo in 316L stainless steel and Si dissolves in 316L and form liquid phase responsible for the densification of the powder compact. Mo addition to austenitic stainless steels has been reported to enhance the mechanical and corrosion properties of the stainless steels [23,24]. Si as sintering additive to stainless steel achieves high sintered density to ensure mechanical and corrosion properties [8,25]. Si form liquid phase at sintering temperatures above 1200 °C, which favors the densification of 316L stainless steel. High density (98.2%) is achieved for 316L P/M specimens containing 5 wt.% $MoSi_2$ content, when sintered at a sintering temperature of 1300 °C.

XMAPs in Fig. 3(d)–(f) shows that increasing $MoSi_2$ content to 10 wt.% clearly increases the Mo phase in the microstructure and Si phase appears in the microstructure in form of round particles. Since Si has low solubility in austenite phase [29,30], it precipitates out as a separate phase in the microstructure (Fig. 3(d)–(f)). The large additions of Si to steels can cause brittleness and hence adversely affect mechanical properties [29]. In our case, the excessive Si precipitated out as separate pure silicon phase. On the other hand, the sintering is carried out in a high vacuum furnace at a vacuum of 1×10^{-2} Pa, it is very less likely to form SiO_2. Hence, the sintered specimens show high tensile strength and ductility (Table 2).

The overview of the mechanical properties of sintered 316L stainless steel with the addition of $MoSi_2$ is given in Table 2. Without $MoSi_2$ addition, the steel sintered at 1300 °C showed hardness as high as 66 HRB. Increase in hardness is observed with increase in $MoSi_2$ addition. This high hardness is due to the increased densification and presence of molybdenum phase in the steel. Hardness value reaches to 93 HRB with 10 wt.% addition of $MoSi_2$ to steel. Table 2 shows the variation of the strength of 316L stainless steel alloy with $MoSi_2$ content. The maximum ultimate tensile strength of 486 MPa and elongation above 20% are achieved with 5 wt.% $MoSi_2$. This high strength and ductility are shown at 98.2% of theoretical density. $MoSi_2$ addition, homogeneous microstructure and less residual porosity have contributed for such high strength and ductility. Ultimate tensile strength and % elongation of 316L stainless steel reduces with increase in $MoSi_2$ addition to 10 wt.%. This is

Table 2
Effect of $MoSi_2$ addition to 316L stainless steel sintered at 1300 °C on the mechanical properties.

Specimen	Tensile strength (MPa)	Elongation (%)	Hardness (HRB)
316L	335 ± 15	14 ± 2	66 ± 2
316L + 1 wt.%	382 ± 15	14 ± 2	69 ± 2
316L + 5 wt.%	486 ± 15	22 ± 2	79 ± 2
316L + 10 wt.%	471 ± 15	16 ± 2	93 ± 2

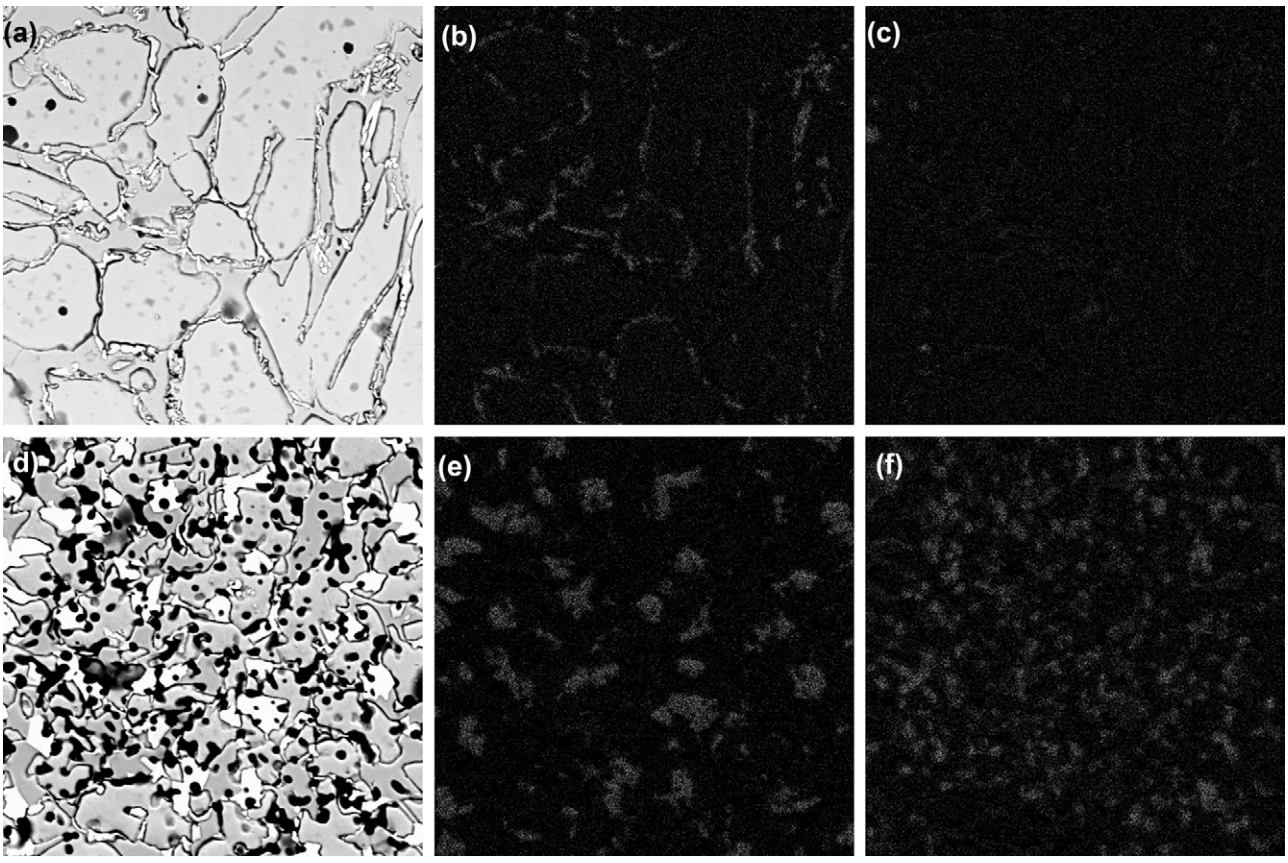

Fig. 3. Microstructure and corresponding XMAPs of Mo and Si of 316L stainless steel sintered at 1300 °C for 60 min (a) with 5 wt.% $MoSi_2$; (b) XMAP of Mo; (c) XMAP of Si; (d) with 10 wt.% $MoSi_2$ at 1300 °C for 60 min; (e) XMAP of Mo; (f) XMAP of Si.

reasonably ascribed to presence of excessive Si in the alloy [8,29]. A clear trend in mechanical properties enhancement with $MoSi_2$ addition is observed. The optimum conditions to achieve a better combination of mechanical properties and high density are 5 wt.% additions of $MoSi_2$ and sintering temperature of 1300 °C.

4. Conclusions

The effect of $MoSi_2$ addition to 316L stainless steel on the sintering behavior, microstructural evolution and mechanical properties was investigated. $MoSi_2$ dissociated into its constituents Mo and Si at the sintering temperature, when added to 316L stainless steel. With increasing $MoSi_2$ content, the sintered density of 316L stainless steel increased and a maximum sintered density of 98.2% of theoretical was achieved with 5 wt.% $MoSi_2$ addition. The microstructure of 316L stainless steel with 10 wt.% $MoSi_2$ content showed precipitates of insoluble Mo and Si phases. Addition of $MoSi_2$ to 316L stainless steel enhanced the sintered density, hardness and ultimate tensile strength of the sintered alloy. Ultimate tensile strength and hardness of sintered 316L stainless steel as high as 486 MPa and 93 HRB were obtained, respectively. The best combination of mechanical properties was achieved with addition of 5 wt.% $MoSi_2$ addition after sintering at 1300 °C for 60 min.

Acknowledgements

F. A. acknowledges F.E. Cui for scanning electron microscopy and financial support from Higher Education Commission of Pakistan.

References

[1] N. Kurgan, R. Varol, Powder Technol. 201 (2010) 242–247.
[2] F. Akhtar, S.J. Guo, K.A. Shah, Powder Metall. 49 (2006) 28–33.
[3] F. Akhtar, J. Mater. Eng. Perform. 16 (2007) 726–729.
[4] H.Ö. Gülsoy, Wear 262 (2007) 491–497.
[5] H.Ö. Gülsoy, M.K. Bilici, Y. Bozkurt, S. Salman, Mater. Des. 28 (2007) 2255–2259.
[6] H.Ö. Gülsoy, Scripta Mater. 52 (2005) 187–192.
[7] X. Yang, S. Guo, J. Iron Steel Res. Int. 15 (2008) 10–14.
[8] M. Youseffi, K.Y. Chong, Powder Metall. 46 (2003) 30–38.
[9] N. Tosangthum, O. Coovattanachai, R. Tongsri, Advances in Powder Metallurgy and Particulate Material, Metal Powder Industries Federation, Princeton, NJ, 2004, Part 5, pp. 51–60.
[10] F. Akhtar, J. Alloys Compd. 459 (2008) 491–497.
[11] F. Akhtar, S. Guo, Acta Mater. 55 (2007) 1467–1477.
[12] F. Akhtar, S. Guo, F. Cui, P. Feng, T. Lin, Mater. Lett. 61 (2007) 189–191.
[13] S. Balaji, A. Upadhyaya, Mater. Chem. Phys. 101 (2007) 310–316.
[14] J. Jain, A.M. Kar, A. Upadhyaya, Mater. Lett. 58 (2004) 2037–2040.
[15] S.N. Patanker, M.J. Tan, Powder Metall. 43 (2000) 350–352.
[16] F. Akhtar, P. Feng, X. Du, A.S. Jawid, J. Tian, S. Guo, Mater. Sci. Eng. A 472 (2008) 324–331.
[17] P. Feng, W. Liu, F. Akhtar, J. Wu, J. Niu, X. Wang, Y. Qiang, Combustion synthesis of $(Mo_1-xCr_x)Si_2$ (x = 0.00–0.30) alloys in SHS mode, Adv. Powder Technol., in press, doi:10.1016/j.apt.2011.01.003.
[18] P. Feng, X. Qu, F. Akhtar, X. Du, H.S. Islam, C. Jia, J. Alloys Compd. 456 (2008) 304–307.
[19] D.E. Jiang, E.A. Carter, Acta Mater. 53 (2005) 4489–4496.
[20] M. Wang, D.B. Bi, W.G. Qin, Vacuum 84 (2010) 1171–1175.
[21] R.J. Brigham, Corrosion 28 (1972) 177–179.
[22] R.J. Brigham, Corros. Sci. 15 (1975) 579–580.
[23] R.J. Brigham, Mater. Perform. 13 (1974) 29–31.
[24] R.J. Brigham, E.W. Tozer, Corrosion 30 (1974) 161–166.
[25] A. Sharon, D. Itzhak, Mater. Sci. Eng. A 157 (1992) 145–149.
[26] S.L. Kang, Sintering: Densification, Grain growth and Microstructure, Elsevier Butterworth–Heinemann, UK, 2005.
[27] B. Weiss, R. Stickler, Metall. Trans. 3 (1972) 871–876.
[28] Y.I. Bil'chugov, N.L. Makarova, A.A. Nazarov, Prot. Met. 37 (2001) 659–664.
[29] W.J. Yuan, R. Li, Q. Shen, L.M. Zhang, Mater. Charact. 58 (2007) 376–379.
[30] O. Kubaschewski, in: H. Okamoto (Ed.), Phase Diagrams of Binary Iron Alloy, ASM International, Materials Park, OH, 1993, pp. 380–381.